IN-WATER NEUTRON AND GAMMA DOSE DETERMINATION

FOR A NEW CF-252 BRACHYTHERAPY SOURCE

A Thesis
Presented to
The Academic Faculty

by

Robert S. Kelm

In Partial Fulfillment
of the Requirements for the Degree
Master of Science in the
George W. Woodruff School of Mechanical Engineering

Georgia Institute of Technology
May 2009

IN-WATER NEUTRON AND GAMMA DOSE DETERMINATION

FOR A NEW CF-252 BRACHYTHERAPY SOURCE

Approved by:

Dr. C.-K. Chris Wang, Advisor
Nuclear and Radiological Engineering
Georgia Institute of Technology

Dr. Nolan E. Hertel
Nuclear and Radiological Engineering
Georgia Institute of Technology

Dr. Sang Hyun Cho
Nuclear and Radiological Engineering
Georgia Institute of Technology

Date Approved: March 9th, 2009

ACKNOWLEDGEMENTS

TABLE OF CONTENTS

LIST OF TABLES

LIST OF FIGURES

SUMMARY

Recently, the <u>O</u>ak <u>R</u>idge <u>N</u>ational <u>L</u>aboratory (ORNL) successfully encapsulated a new generation of medical grade ^{252}Cf sources having intensities and size comparable to that of the widely used <u>h</u>igh-<u>d</u>ose-<u>r</u>ate (HDR) ^{192}Ir brachytherapy sources. Advent of the new sources, therefore, marked a new era for ^{252}Cf-based <u>n</u>eutron <u>b</u>rachy<u>t</u>herapy (NBT). As part of source calibration and characterization process, a study has been conducted at Georgia Tech lately on determining the neutron and gamma dose rates in water surrounding the new ^{252}Cf source. A Lucite-walled water phantom was built for this study. The neutron and gamma dose rates were determined both by ion chamber measurements and by Monte Carlo code MCNP. The results show that the measured neutron absorbed dose rates were approximately 25% lower than that predicted by MCNP for all dose positions in water, suggesting that the ^{252}Cf content of the new source is actually 25% lower than the ORNL's estimate. The measured gamma absorbed dose rates in water, on the contrary, are higher than that predicted by MCNP. The differences between the measured and MCNP-predicted gamma doses are not uniform for all dose positions; they are most pronounced (~a factor of two) at the distance of 1 cm, and fall to approximately 30% at distances 2 cm and beyond. These results suggest that the spectrum of gamma rays emitted from the new ^{252}Cf source may contain significantly more low-energy gamma rays than the previously published spectrum used in MCNP.

CHAPTER 1

INTRODUCTION

The clinical advantages of ^{252}Cf-based neutron brachytherapy therapy (NBT) over the conventional x- or gamma-ray treatment in treating radioresistant cancers were first demonstrated in the 1980's in the US [1], and more recently in China [2]. Because the commercially available ^{252}Cf sources are too large in size, the clinical applications of NBT so far are limited to a small number of intracavitary treatments of cervical cancers. Recently, under a Cooperative Research and Development Agreement (CRADA) with Isotron, Inc.(a start-up company located in Alpharetta, Georgia), the Oak Ridge National Laboratory (ORNL) successfully encapsulated a new generation of medical grade ^{252}Cf sources - referred as Isotron sources hereafter [3]. The outside dimensions of the Isotron source capsule are 1.1 mm in diameter and 8 mm in length. The active length of the source is 5 mm. The capsule wall thickness is 0.2 mm, and it is made of platinum-10% iridium alloy. At the time of encapsulation (October 2002), the average ^{252}Cf content in each source seed was estimated to be approximately 90 µg, which is 200 times of the content in the old sources of a comparable physical size. The small size of the new sources allow them to be used with remote high-dose-rate (HDR) afterloading systems comparable to current ones already in use for ^{192}Ir interstitial gamma brachytherapy. Advent of the Isotron sources, thus, mark a new era for NBT.

The Isotron sources, however, must be properly calibrated and characterized before they can be widely used to treat patients. As such, in October 2007, one Isotron source was shipped from ORNL to Georgia Tech where the in-water dose measurements were conducted. Because ^{252}Cf emits both neutrons and gamma rays and because neutrons are much more effective than gamma rays in causing biological damages to cells, it is essential that neutron and gamma doses are determined separately. The neutron and

gamma doses in water were determined by computations based on the Monte Carlo code MCNP [4] and by measurements based on the dual ion chamber method [5]. Chapter 2 provides detailed description of the Isotron source. Chapters 3 and 4 describe the computational method and the measurement method, respectively. Chapter 5 shows the results of the two methods and discusses the discrepancies. Chapter 6 provides conclusions and suggests future work.

CHAPTER 2

DESCRIPTION OF THE ISOTRON SOURCE

Cf-252 emits neutrons, gamma rays, beta particles, and alpha particles. Cf-252 decays by both alpha emission (96.91% probability) and spontaneous fission (3.09% probability) for a combined half-life of 2.645 years. Cf-252 has a specific activity of 0.5362 mCi/µg and a neutron emission rate of 2.31434×10^6 neutrons/s/µg. Cf-252's spontaneous fission neutron spectrum is similar to a fission reactor's in shape with an average energy of 2.1 MeV and a most probable energy of 0.7 MeV [6].

A replica of the Isotron source is pictured below in Figure 2.1. The source was fabricated in October of 2002 at ORNL and shipped to Georgia Tech in October of 2007. The source fabrication information including the isotropic composition of the Californium is shown in Table 2.1. The source has an outside diameter of 1.1 mm and a length of 8 mm. The wall material is 0.2 mm thick and consists of a platinum-10% iridium alloy. The casing cylinder is welded shut on one end and crimped to a 3 inch stainless steel cable on the other. Inside of the Pt-10%Ir casing is a free floating 5 mm long Pd-Cf_2O_3 cermet wire. The wire has an approximate diameter of 0.5 mm. The amount of ^{252}Cf in the Isotron source was measured at ORNL by surrounding the source with three ^{235}U fission chambers. The neutron count rates of the Isotron source were then compared with the count rates produced by a NIST (National Institute of Standards and Technology) calibrated source of which the ^{252}Cf quantity was determined with the Manganese Sulfate ($MnSO_4$) Bath Method [7]. The ratio of this comparison determined the quantity of ^{252}Cf contained in the Isotron source. It should be noted that the quantity of ^{252}Cf contained in the NIST-calibrated source has an inherent uncertainty of approximately 3%. The ^{252}Cf content of the source is listed as 24.22 µg as of September

30, 2007. This value was obtained by using Cf-252's half-life to decay the original measured amount of ^{252}Cf.

Figure 2.1. Photo of an Isotron source.

Table 2.1. Source fabrication information provided by ORNL

Neutron Source	ISO-2
Sample Identification	CX-CF-669
Date of Analysis	March 8, 2001
	Isotopic Composition
Nuclide	(atom %)
Cf-249	1.87
Cf-250	9.10
Cf-251	2.78
Cf-252	86.13
Cf-253	0.001
Cf-254	0.008
Date of Final Purification	October 4, 2002
Date of Californium Assay	October 4, 2002
Calculated Fraction of Neutrons from Cf-252	0.99800[a]
Cf-252 Content, μg	24.22[a]

[a]Value decayed to September 30, 2007

CHAPTER 3

COMPUTATIONAL STUDY

3.1 Introduction to MCNP

In this study, the Monte Carlo code MCNP-5 was used to calculate neutron and gamma-ray doses in water at various distances from the Isotron source. MCNP is a general purpose Monte Carlo N-Particle code developed and maintained by Los Alamos National Laboratory. It is the most widely used computer code for neutron/gamma-ray/electron coupled transport simulations and is accepted as a benchmark by the international community. MCNP simulates individual particles and tracks them from birth (source) till death (absorption, escape, etc) based on physics rules and probabilities given by tabulated transport data (e.g. the neutron and gamma-ray cross section data libraries). Specific quantities such as particle fluence and absorbed dose in specified places (tallies or detectors) are obtained by averaging the contributions of a large number of particles. The final results (i.e. particle fluences or absorbed doses) of MCNP are normalized to a single source particle. Because of the statistical nature of the Monte Carlo method, MCNP calculations often require to run many millions (or even billions) of particles to achieve statistically meaningful results that have uncertainties less than a few percent.

3.2 The MCNP Model

MCNP-5 was used to model the Isotron source in a water phantom. Three separate MCNP runs were required to accurately determine each of the three dose components – i.e. that of neutrons, primary gamma-rays, and secondary gamma-rays.

6

The secondary gamma-rays are mainly produced by thermal neutron capture reactions of $^1H(n,\gamma)^2H$ in water. While in principle it is possible to obtain both neutron and secondary gamma doses in a single MCNP run. In practice, however, tallying gamma dose requires carrying out electron transport calculations, which significantly increases computational time. As such, neutron and secondary gamma doses were obtained with separate MCNP runs.

Truncated sample input files for all three MCNP runs can be found in Appendix A. The three calculations are identical in geometry and materials. In this geometry, the Isotron source is positioned at the center of a water phantom which is 20 cm in height and 20 cm in diameter. The absorbed doses at various distances from the source were obtained by the "ring" tallies (or detectors). The ring detectors take advantage of the symmetry of the source-to-detector geometry making the seemingly small detector volumes significantly larger, which in turn, allow the results to converge more quickly. A 2-dimensional r-z display of the geometry modeled by MCNP is shown in Figure 3.1.
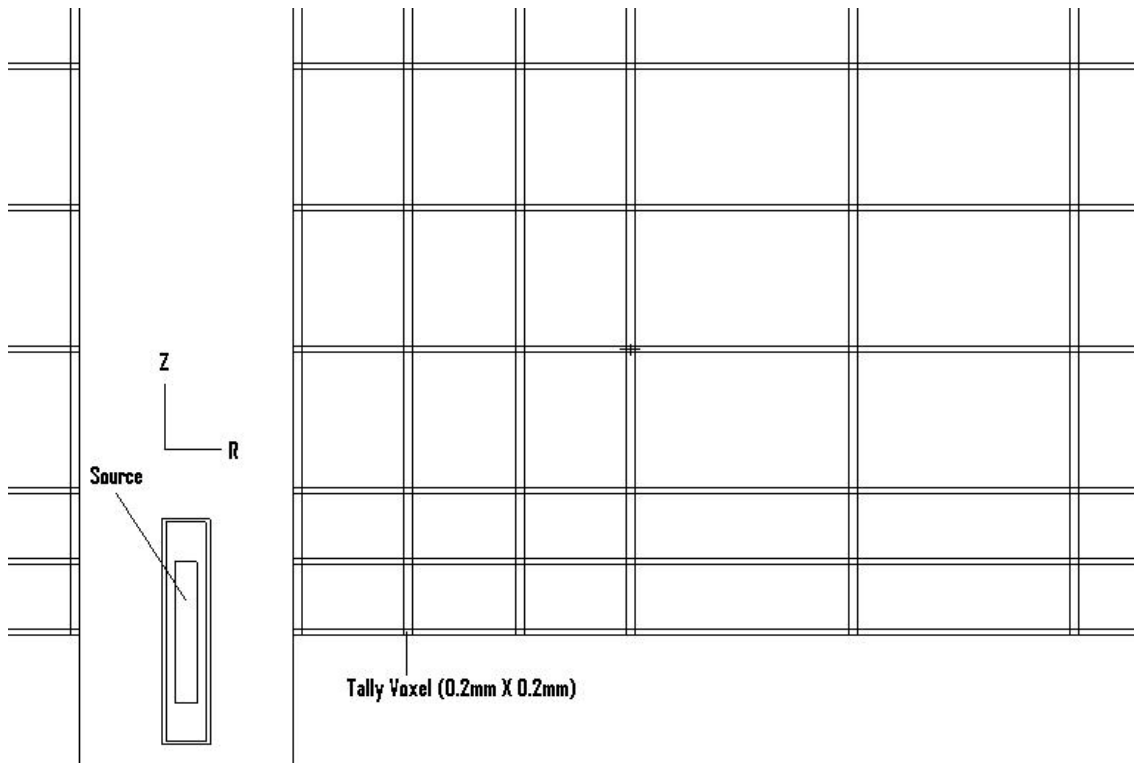

Figure 3.1. The 2-D (*r-z*) display of source-and-tally geometry modeled by MCNP.

7

As shown in Fig. 3.1, the detector volumes being tallied for absorbed doses are shown as the small voxels at the intersections of radial (*r*) and axial (*z*) lines. These voxels have a width of 0.2 mm in both radial and axial directions. As mentioned, because the voxels are symmetric with respect to the source centerline, the actual volume of a voxel being tallied (i.e. the detector volume) is approximately $2\pi r (0.2\,mm)^2$, where *r* is the radial distance of the voxel from the source centerline. Because the detector volume is small and because the probability for a source neutron to reach a detector rapidly decreases as the distance of the detector from the source increases, the computational time for a MCNP run to obtain neutron absorbed doses is dictated by the accuracy of distant detectors. For example, the neutron absorbed doses at distances greater than 4 cm converge so slowly that it is impossible to obtain statistically meaningful results with any reasonable amount of computational time. The computational time for a MCNP run to obtain primary gamma doses is less dictated by the accuracy of distant detectors. This is because gamma photons have much greater mean free paths than that of neutrons and, thus, have higher probabilities to reach distant detectors. Finally, the computational time for a MCNP run to obtain secondary gamma doses is almost independent of detector locations. This is because the spatial distribution of thermal neutron-induced secondary gamma photons is fairly uniform up to at least 5 cm from the source.

The energy of a neutron emitted from Cf-252 is often modeled as either a Maxwellian or Watt fission spectrum. MCNP manual recommends using a Watt fission spectrum in estimating the fission spectrum of Cf-252 [4]. However, it does not explain why nor provide references for this recommendation. In fact, all recent published studies that model a Cf-252 needle source recommend an isotropic Maxwellian neutron energy spectrum described by Equation 3.1 below [8].

$$N(E) = C\,e^{-E/1.42}E^{0.5} \tag{3.1}$$

While the Maxwellian spectrum was thought to be more representative than a Watt spectrum, the supporting references mainly deal with examining the applicability of the Maxwellian for neutron energies above 5 MeV [9,10]. Since most Cf-252 neutrons are at energies below 5 MeV, there is no reason to believe that Maxwellian spectrum would produce more accurate neutron doses in water. As such, in this study neutron doses were obtained with two separate MCNP runs, one uses the Maxwellian spectrum of Eq. 3.1 and the other uses the Watt spectrum described by Eq. 3.2.

$$N(E) = C\,e^{-E/1.025}\,Sinh(2.926E)^{0.5} \tag{3.2}$$

The unit of E in both equations is in MeV. The results obtained from two separate neutron dose calculations would provide the uncertainties of neutron doses caused by the uncertainties associated with the source neutron spectrum.

Neutron absorbed doses in at various positions in water were estimated using F6 tallies, which is an estimate of kerma, or kinetic energy of charged particles released per unit mass in a material. Kerma is an excellent approximation of absorbed dose for neutrons because a large majority of the charged particles (mainly recoil protons) that contribute to the absorbed dose have very short ranges (<0.2 mm) so that charged particle equilibrium (CPE) is well established in each tally volume. In MCNP, a F6 tally result is obtained by multiplying energy-dependent neutron fluences with the corresponding neutron kerma factors and then summing together. Because the kerma factors are pre-calculated values, the MCNP run for obtaining neutron doses converges rather quickly. In this study, 10^8 particles were run when performing neutron dose calculations.

As mentioned, two separate MCNP runs were made for gamma dose calculations – one for primary gamma dose (from prompt and decay gammas) and one for secondary gamma dose (from n,γ reactions).   The primary gamma dose calculation uses a source gamma spectrum approximating that of Cf-252's prompt fission and equilibrium fission product gamma rays. Table 3.1 shows the primary gamma source spectrum used in

MCNP. [6]   The secondary gamma dose calculation uses the Maxwellian spectrum (Eq. 3.1) to initiate source neutrons. Because the Compton scattered electrons have relatively long ranges (a few millimeters) in water, kerma is no longer a good approximation of absorbed dose. To accurately calculate absorbed gamma doses, the MCNP runs must carry out the transport of electrons.   Because each electron history includes a large number of collisions, it takes much more computational time for MCNP to carry out gamma dose calculations. The *F8 tally was used to obtain the absorbed gamma dose. The *F8 tally records energy deposition in a cell by following each individual electron and subtracting the electron's energy leaving the cell from its energy entering the cell. 5 x 10^7 particles were run for each gamma dose calculation.

Table 3.1. Primary gamma source spectrum [6]

Group	E_{high} (MeV)	E_{low} (MeV)	Intensity (γ/s/μg)	Total Energy (MeV/s/μg)
1	10.00	8.00	9.825E+02	8.85E+03
2	8.00	6.50	4.627E+03	3.35E+04
3	6.50	5.00	2.358E+04	1.36E+05
4	5.00	4.00	5.875E+04	2.65E+05
5	4.00	3.00	1.740E+05	6.08E+05
6	3.00	2.50	1.937E+05	5.32E+05
7	2.50	2.00	3.338E+05	7.52E+05
8	2.00	1.66	5.507E+05	1.01E+06
9	1.66	1.33	0.000E+00	0.00E+00
10	1.33	1.00	1.264E+06	1.47E+06
11	1.00	0.80	5.630E-02	5.07E-02
12	0.80	0.60	3.073E+06	2.15E+06
13	0.60	0.40	5.242E-01	2.62E-01
14	0.40	0.30	7.587E+03	2.65E+03
15	0.30	0.20	3.540E+06	8.85E+05
16	0.20	0.10	2.515E+03	3.77E+02
17	0.10	0.05	1.613E+03	1.21E+02
18	0.05	0.01	7.300E+05	2.18E+04
Total:	----	----	9.959E+06	7.88E+06

CHAPTER 4

MEASUREMENT METHOD

4.1 The Two-Ion Chamber Method

A common method to measure neutron and gamma-ray dose contributions in a mixed neutron and gamma field is to use two ion chambers having different neutron and gamma sensitivities. Ion chambers work by applying a voltage across a gas volume and collecting all the charge associated with direct ionization occurring within the gas volume. These ionizations are primarily from secondary charged particles (i.e. electrons and protons) originating from the chamber wall. As such, ion chambers with walls made of different materials may have very different neutron and gamma sensitivities.

To measure neutron and gamma absorbed doses in water surrounding the Isotron source, two miniature free air thimble ion chambers from Standard Imaging, Inc. were used. The product names of the two chambers are T1 and M1. The wall of T1 is constructed from tissue equivalent A-150 plastic and is sensitive to both neutron and gamma radiation. The wall of M1 is constructed from magnesium and is predominately sensitive to gamma-rays. Both chambers are identical in every other way. The M1 ion chamber along with the electrometer used in the measurements is shown in Figure 4.1. Both ion chambers have a collecting volume of 0.056 cm^3. The outer diameter of the chambers is 6.0 mm with a wall thickness of 1 mm. Attached to the chamber is a vent tube and stem. The ion chambers are attached to a 1.5 meter low-noise triaxial cable. The cable passes bias voltage and collected charge to the Max 4000 electrometer (also manufactured by Standard Imaging, Inc.). The electrometer is capable of reading an electrical current as low as 0.01 pA, and the total leakage current of the system (i.e. electrometer plus triaxial capable) is less than 0.003 pA.
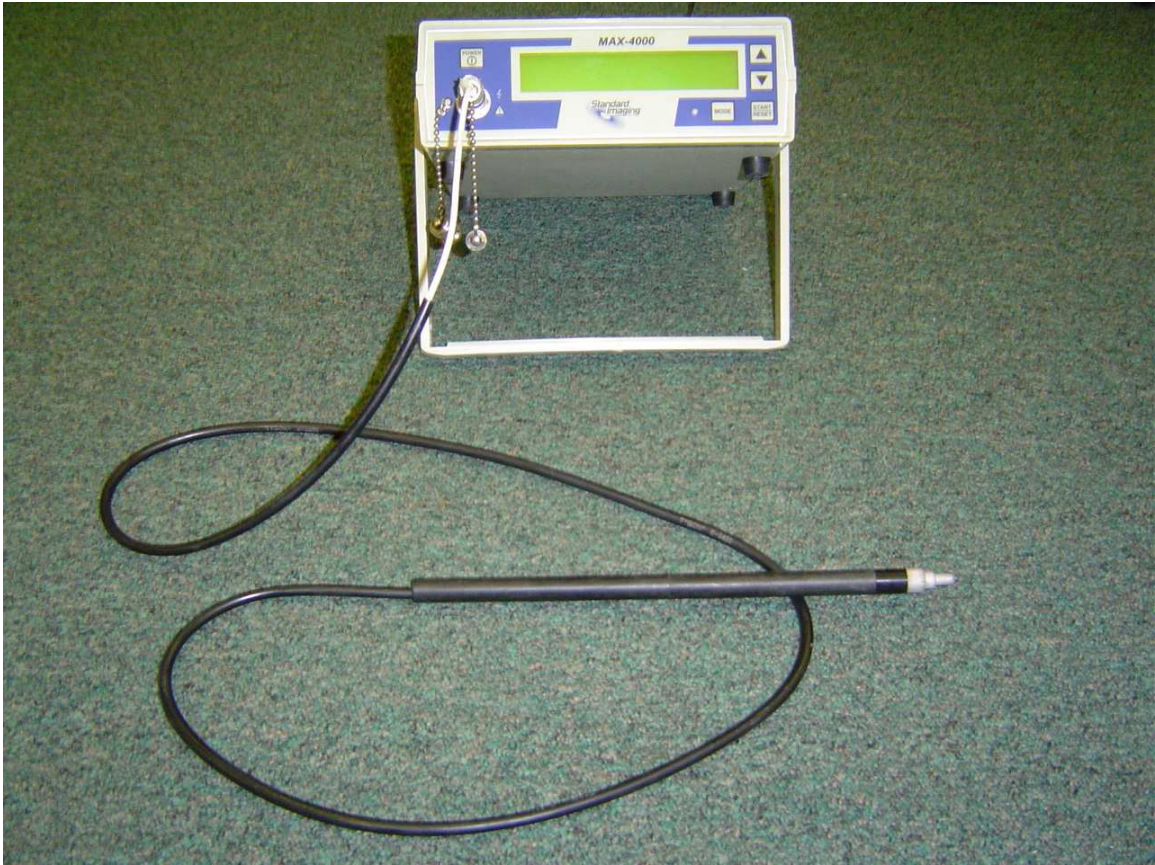
Figure 4.1. M1 ion chamber connected to Max-4000 electrometer.

An ion chamber's response to mixed gamma and neutron radiation can be described by the following equations. [11, 12]

$$Q_{n,\gamma} = AD_{\gamma} + BD_{n} \tag{4.1}$$

or

$$\frac{Q_{n,\gamma}}{A} = D_{\gamma} + \frac{B}{A}D_{n} \tag{4.2}$$

Where:

$Q_{n,\gamma}$ =   total response by the detector in the mixed field.

A =   response per unit absorbed dose due to gamma-rays

B =   response per unit absorbed dose due to neutrons

D_{γ} =   gamma absorbed dose

D_{n} =   neutron absorbed dose

Basically A and B are calibration factors describing the sensitivity of the ion chamber to the corresponding radiation. The calibration factor for gamma rays can be obtained using a known Co-60 free-space exposure rate. Under the condition of electronic equilibrium, the absorbed dose at the center of a sphere of tissue, 0.52 g/cm^2 in radius, due to some free-space exposure can be expressed as:

$$D_{\gamma} = \beta A_{eq} X (\frac{\overline{W}}{e})_{air} (\frac{\mu_{en}}{\rho})_{a}^{tiss} \tag{4.3}$$

Where:

X =   free-space exposure (C/kg)

β =   1.003

A_{eq} =   photon attenuation to the center of the sphere $=$ 0.988

$$(\frac{\overline{W}}{e})_{air} = 33.97 \text{ J/C}$$

$$(\frac{\mu_{en}}{\rho})_{a}^{tiss} = \text{ mass energy absorption coefficient ratio of tissue to air} = 1.102$$

Plugging in values for the variables, equation (4.3) is reduced to:

$$D_\gamma = 37.1X \, (Gy) \tag{4.4}$$

Similarly, if a gamma ray-only radiation field is present such as Co-60, equation (4.2) can be simplified and split up into the following two equations for T1 and M1, respectively:

$$A_{TE} = \frac{Q_\gamma^{TE}}{D_\gamma}(C/Gy) \tag{4.5}$$

$$A_{Mag} = \frac{Q_\gamma^{Mag}}{D_\gamma}(C/Gy) \tag{4.6}$$

The $\frac{B}{A}$ ratios for T1 and M1 needed to complete equation (4.2) are shown in Figure 4.2. [13]
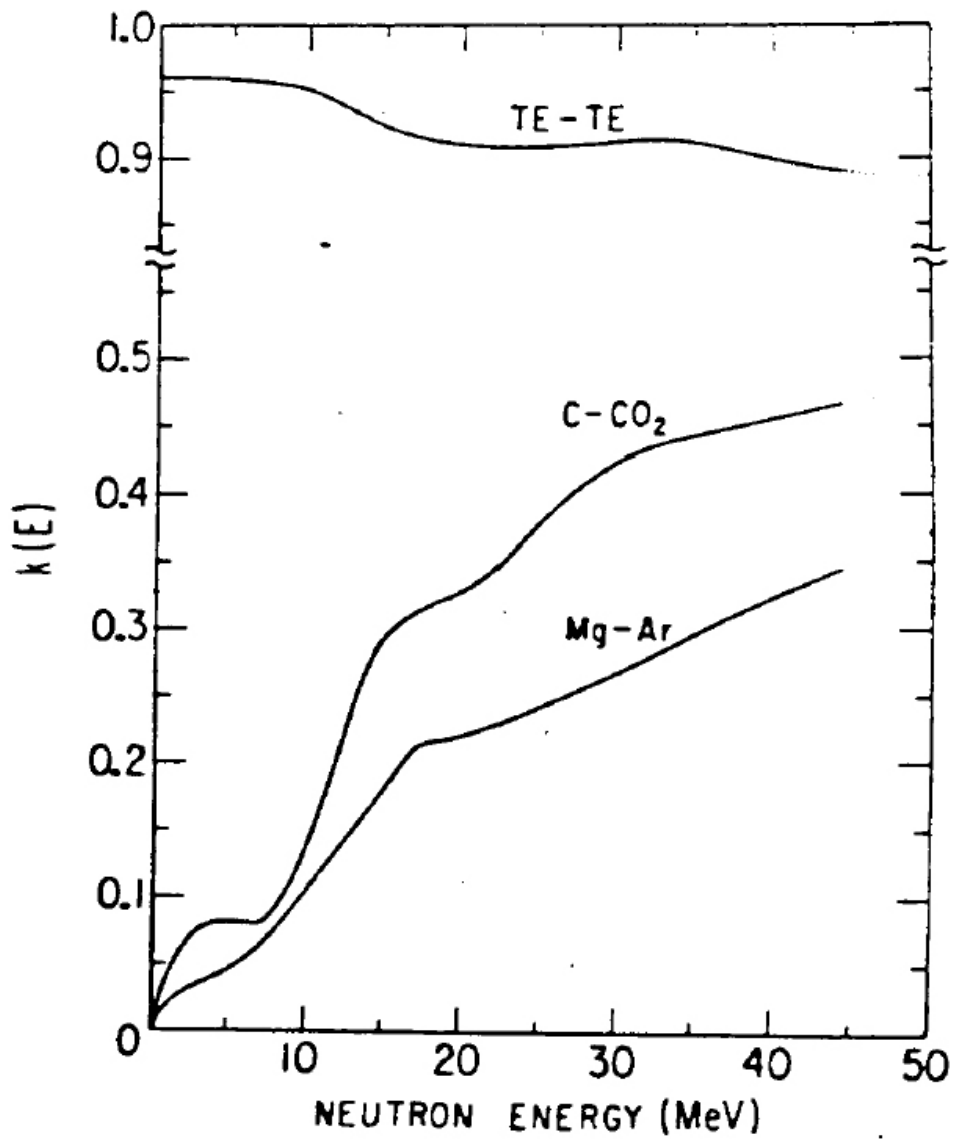
Figure 4.2. Relative neutron response - B/A values versus neutron energy.

4.2 Calibration and Verification of Ion Chambers

The gamma responses (i.e. *A* values of equation (4.1)) of the two ion chambers M1 and T1 were previously calibrated at Georgia Tech Neely Research Center in 2005, and a NIST (National Institute of Standards and Technology) traceable Co-60 source was used in that calibration. The calibration yielded *A* values of $15.67 \pm 4.4\%$ pC/cGy for T1 and $18.2 \pm 2.68\%$ pC/cGy for M1. [12] Since Cf-252's neutron spectrum has an average energy of approximately 2 MeV, reasonable *B/A* ratios for T1 and M1 from Figure 4.2 can be obtained as 0.97 and 0.025, respectively. Substituting these values into equation (4.2) for both T1 and M1 yields the following equations:

$$\frac{Q_{n,\gamma}^{T1}}{15.67\,pc/cGy} = D_\gamma + 0.97D_n \tag{4.7}$$

$$\frac{Q_{n,\gamma}^{M1}}{18.2\,pc/cGy} = D_\gamma + 0.025D_n \tag{4.8}$$

Because the NIST-traceable Co-60 calibration was about three years old at the time of the Isotron source measurements and because Standard Imaging, Inc. recommends calibrating ion chambers and electrometers every two years, the two ion chambers were calibrated for the second time in February, 2008. Because the Co-60 source used at Georgia Tech in 2005 had been returned to the Department of Energy, the second calibration was done with the Varian Trilogy Unit (a linac) at Emory University Radiation Oncology Department. The linear accelerator was operated at a 6 million volt acceleration potential producing x-rays with an approximate average energy of 2 MeV. The beam intensity is regularly calibrated by a PTW Farmer's unit. To perform the calibration of the two ion chambers a water phantom supplied by Emory was used. An ion chamber placed in the water phantom at a distance of 10 cm from the wall facing the

linac beam. The distance between the linac source and the phantom surface was 100 cm. The ion chamber was centered (laser guided) in the center of the 10 cm x 10 cm beam. This set up can be seen in Figure 4.3. To make sure that the ion chamber's reading are independent of dose rate, 0.335 Gy was given over two periods of 5 seconds and 30 seconds for each chamber. The results are shown in Table 4.1. As shown, the *A* values for T1 and M1 are in full agreement with the values previously obtained with the NIST-traceable Co-60 gamma source.
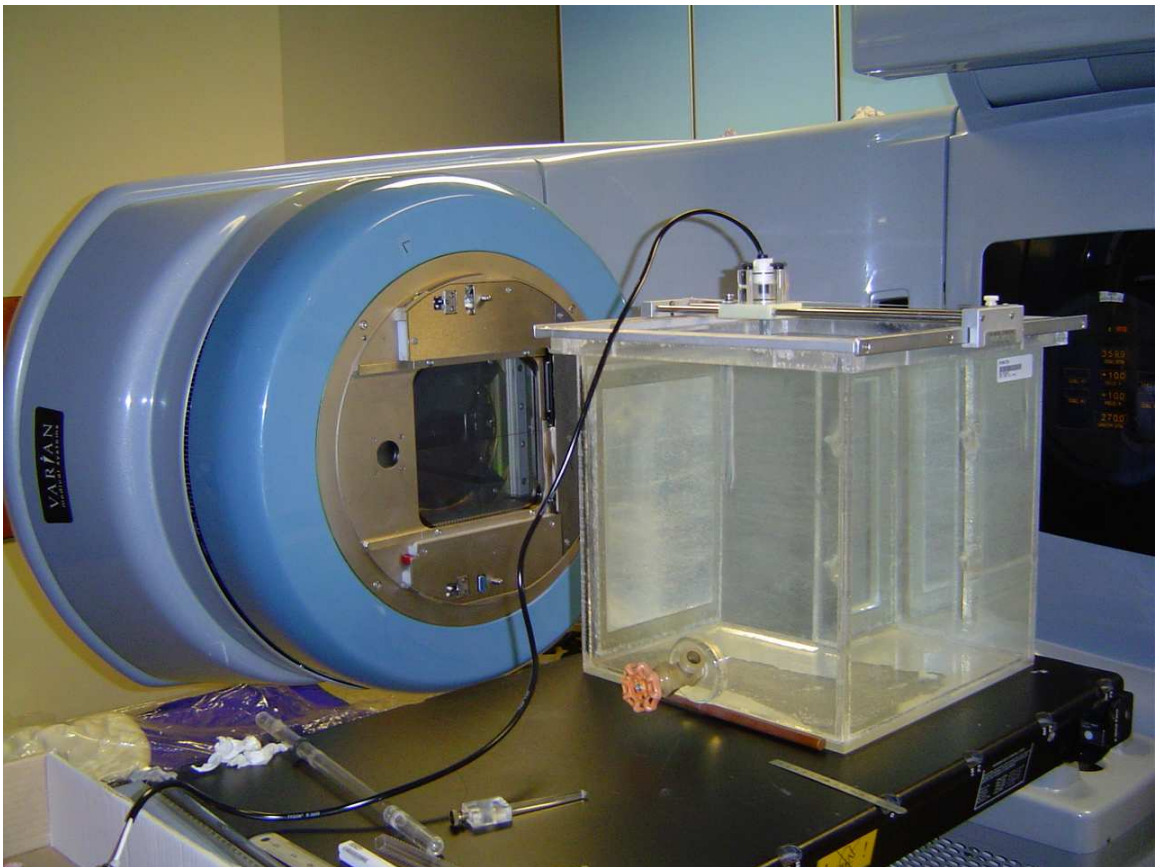
Figure 4.3. T1 in water phantom in front of Emory's Trilogy unit.

Table 4.1. Calibration data obtained at Emory.

T1 Ion Chamber Dose (Gy)	Time	Measured Charge (pC)	Mean Charge (pC)	Deviation (pC)	Standard Deviation (pC)	A_{TE} (pC/cGy)
0.335	5 sec	533.0	533.65	-0.65	1.40	15.93
0.335	5 sec	532.0		-1.65		
0.335	30 sec	534.6		0.95		
0.335	30 sec	535.0		1.35		
M1 Ion Chamber Dose (Gy)	Time	Measured Charge (pC)	Mean Charge (pC)	Deviation (pC)	Standard Deviation (pC)	A_{Mag} (pC/cGy)
0.335	5 sec	613.0	612.25	0.75	1.23	18.28
0.335	5 sec	613.5		1.25		
0.335	30 sec	610.8		-1.45		
0.335	30 sec	611.7		-0.55		

4.3 Experimental Setup

Because the Isotron source intensity was fairly strong, it was necessary to set up the experiment behind a concrete wall to minimize the unnecessary personnel exposure. A water phantom and a remotely controlled positioner were used in the setup. The water phantom is a 30 cm x 30 cm x 30 cm acrylic box made of five 0.635 cm thick 30 cm x 30 cm acrylic plates fused together. The two-dimensional high precision positioner (shown in Figure 4.4) uses two Newport motorized actuators, one in the vertical (axial) and one in the horizontal (transverse) direction. The horizontal motor pushes a sled in relation to the base of the positioner which sits on top of a Plexiglas cover on top of the water phantom. The vertical motor pushes a sled attached to the horizontal sled as a base. This combination of sleds and motors allows the positioner to move the ion chambers freely in the horizontal and vertical directions relative to the phantom. The motors are controlled remotely using a variable voltage controller. Attached to each sled is a plastic caliper

accurate to one tenth of a millimeter. Attached to the vertical sled is the ion chamber holder. An ion chamber is held in place by two plastic zip-ties. Held by the stem, the ion chamber extends into the phantom through a cutout in the Plexiglas cover. An aluminum fixture is attached to the bottom of the Plexiglas cover to hold the plastic catheter where the source is in. The Plexiglas cover has a hole drilled to allow the source to be lowered into place. The catheter is approximately 19.0 cm long and sealed at one end with silicone. JB-weld was used to seal the catheter at first, but was found to leak after prolonged exposure to radiation.
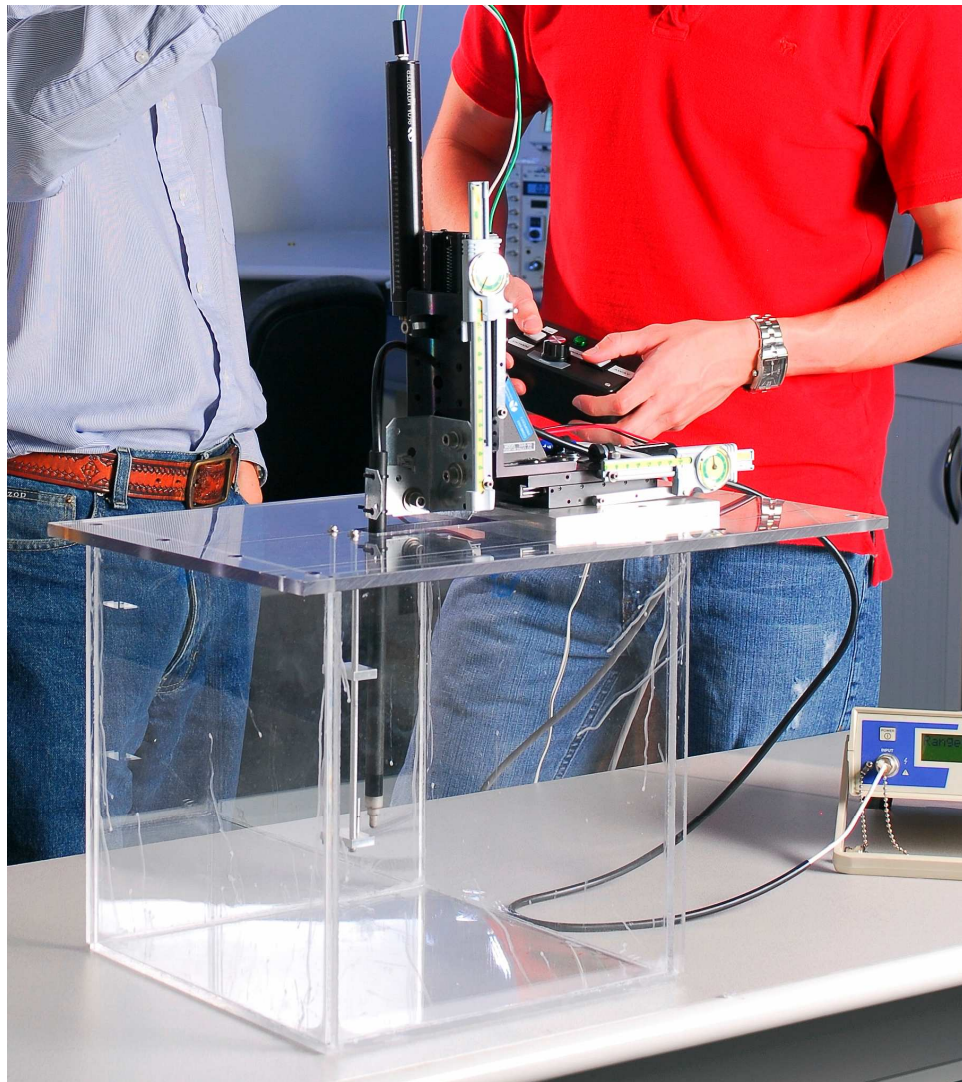
Figure 4.4. Water phantom with two-dimensional positioner.

The measurement took place within the RCZ (radiation control zone) of the Neely Building at Georgia Tech. The overall set-up can be seen in Figure 4.5 with the phantom and source on the left and the operator's working area on the right separated by a thick concrete wall. Figure 4.6 shows the positioner and ion chamber in place with CCTV cameras focused on each of the positioner's calipers. The phantom was filled with de-ionized water. As shown, the triaxial cable leaving the ion chamber enters a hole in the concrete wall between the experimental area and the operator area. This passage allowed the triaxial cable to reach the electrometer (in the operator area) without an extension. Figure 4.7 shows the operator area where the electrometer, monitors displaying the positioner's calipers, and the positioner's control box can be seen.

Figure 4.5. Overall setup of the experiment.

Figure 4.6. Detailed view of the water phantom system in use.

Figure 4.7. The operator area.

The following procedure was used to conduct the measurements for T1 and M1. All source movements were conducted under the supervision of health physics staff from Georgia Tech's Office of Radiological Safety following strict safety procedures not detailed below.

1.   Set up water phantom, CCTV cameras and monitors.

2.   Tape latex sheath (condom) over detector protecting it from the water.

3   Submerge detector in water phantom and fasten stem of detector to the positioner.

4.   Plug MAX-4000 into wall socket and warm up for 10 minutes.

5   Perform a Zero adjustment of the electrometer.

6.   Connect the ion chamber's triaxial cable to the electrometer.

7.   Raise the bias voltage to 300 volts and wait 10 minutes for system stabilization.

8.   Perform a zero adjustment of the electrometer plus detector.

9.   Open the Cf-252 transport cask and remove the catheter containing the source with the handling tool.

10.   Quickly insert the tube containing the source into the water phantom, making sure to line up the tube with the aluminum holder underwater.

11.   Use the positioner's controls to move the ion chamber as close as possible to the source.

12.   Find the source center plane (when the detector is parallel to the source) by moving the detector axially up and down while taking measurements of the charge. The center plane is where the reading is the highest.

13.   With traverse and axial positions now known, take three 300 second measurements recording the charge each time.

14.   Move the detector using the remote and CCTV cameras to the next desired position and repeat measurements.

15.   Once finished with the measurements or with the allotted time for that day, remove the source and take three 600 second background/leakage measurements. Do not remove the ion chamber until all measurements for that chamber have been completed.

Steps 11 and 12 from above calibrate the ion chambers in position relative to the source. The two ion chambers must take measurements at the same positions to be able to separate the neutron and gamma ray dose contributions. In step 11, to make sure the T1 and M1 were taken in the same traverse positions (horizontal) from the source, each detector was started at the closest possible position to the source. Using a digital caliper, this distance was measured to be 1.085 cm. For T1, this position was at the caliper reading of 139.8 mm. For M1, the position was 138.5 mm. The two numbers are different because the positioner was moved while changing detectors. In step 12, to find the source center plane, at their closest traverse position each detector was moved up and down axially while taking charge measurements. Graphs of this axial position calibration can be viewed in Figures 4.8 and 4.9. As shown, the center plane for T1 and M1 were found to be 104.0 mm and 108.0 mm, respectively. Combining the traverse and axial calibration, conversions from caliper reading to actual distances from the source are provided in Table 4.2.
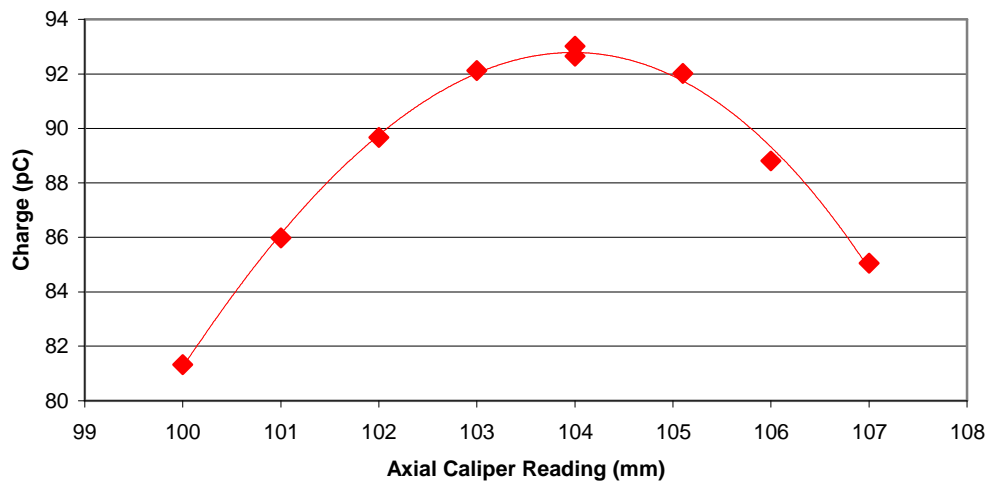
Figure 4.8. Centerline calibration for T1 measurements.
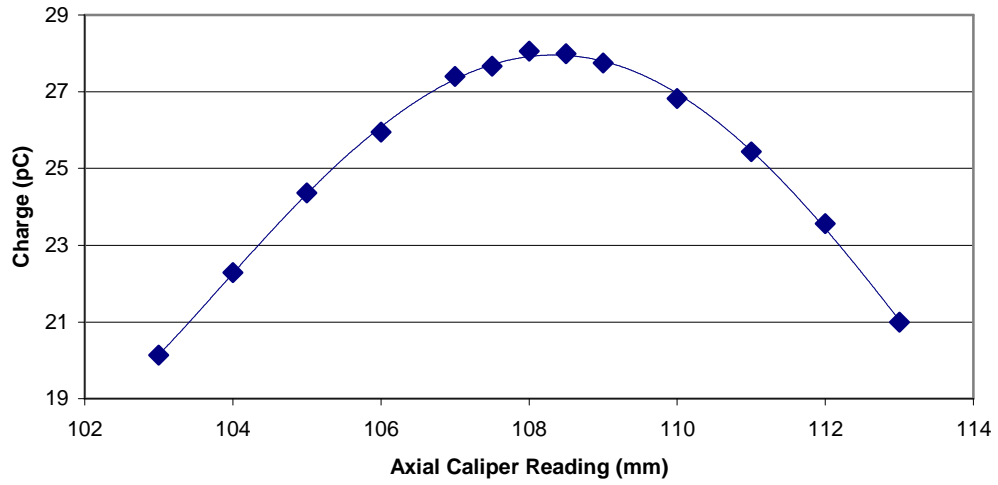
Figure 4.9. Centerline calibration for M1 measurements.

Table 4.2. T1 and M1 caliper readings to actual distance along axis.

T1 Ion Chamber				
Transverse Caliper Reading (mm)	Transverse Distance From Source (cm)		Axial Caliper Reading (mm)	Axial distance from Source (cm)
139.80	1.085		104.00	0
134.80	1.585		99.00	0.5
129.80	2.085		94.00	1
124.80	2.585		89.00	1.5
119.80	3.085		84.00	2
114.80	3.585			
M1 Ion Chamber				
Transverse Caliper Reading (mm)	Transverse Distance From Source (cm)		Axial Caliper Reading (mm)	Axial distance from Source (cm)
138.50	1.085		108.00	0
133.50	1.585		103.00	0.5
128.50	2.085		98.00	1
123.50	2.585		93.00	1.5
118.50	3.085		88.00	2
113.50	3.585			

CHAPTER 5

RESULTS AND DISCUSSION

5.1 Computational Results

Figure 5.1 shows the 3-dimensional neutron dose distribution in water obtained from MCNP. Figure 5.2 shows the neutron isodose contours surrounding the source. In both figures the absorbed dose is displayed as factors normalized to the dose at a distance of 1 cm along the traverse axis of the source. Note that in Figure 5.1, the scale for absorbed dose is logarithmic. As shown, the neutron dose gradient is extremely sharp at distances near the source and falls off rapidly as distance increases. Graphs for gamma dose rates are not shown, but would appear similar.

To verify the success of the above results, comparisons with previous published studies [8,14,15] are displayed in Tables 5.1 and 5.2 for both neutron and gamma-ray absorbed dose rates. The new results presented in Tables 5.1 and 5.2 have an uncertainty of less than 1 %. In Table 5.1, the MCNP neutron results of this study agree well especially with Krishnaswamy's calculation of a 0.4 cm active length source and Rivard's point source calculation. Discrepancies in values can be attributed to the differences in the models. Krishnaswamy's model used a Watt fission spectrum for the neutron source. This spectrum over estimates the absorbed dose compared to the Maxwellian spectrum by 4-7% over 0.5 to 5 cm distance from the source. The difference in source active lengths of 0.4 to 0.5 cm results in at most a 3% difference. The Krishnaswamy study used larger voxels underestimating the dose near the source by averaging over a sharp dose gradient. In addition, the Krishnaswamy study was based on absorbed dose in tissue where results of this study are based on dose in water. Fewer differences exist between Rivard's calculation and the current one. Both use a

Maxwellian spectrum and small voxels. Both are based on neutron kerma of water in a water phantom. The main difference between the two is geometry. Rivard's calculations were based on spherical geometry and a point source as opposed to the cylindrical geometry and a needle source modeled in this study. This accounts for why Rivard's values are greater at 0.5 cm and converge to the current results as the distance from the source increases.

Table 5.2 shows a good agreement in gamma doses between the current MCNP results and previous works. This is despite a big uncertainty associated with the gamma source spectrum. It is likely (but unclear) that Krishnaswamy used the gamma spectrum available from the Cf-252 Shielding Guide [16] published in 1971. This study is based on the newer gamma spectrum published by ORNL in 2000 [6]. The newer spectrum contains significantly less low-energy gamma rays and slightly greater high-energy gamma rays for a combined difference of approximately 30% less intensity and total energy. The actual difference to the absorbed dose calculations using these two different spectra was not studied.
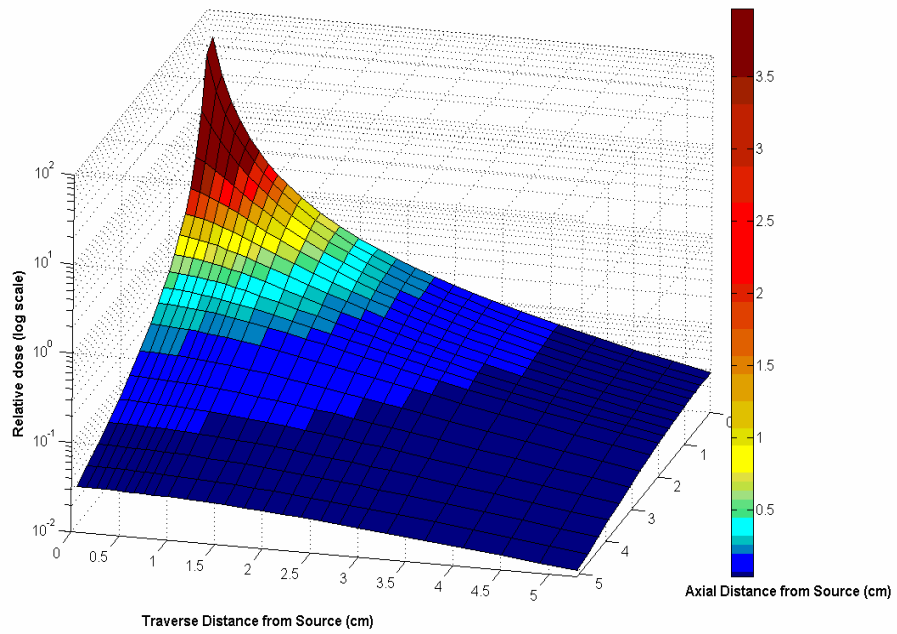
Figure 5.1.   Neutron dose presented in 3-D normalized as factors of the dose 1 cm traverse the source.
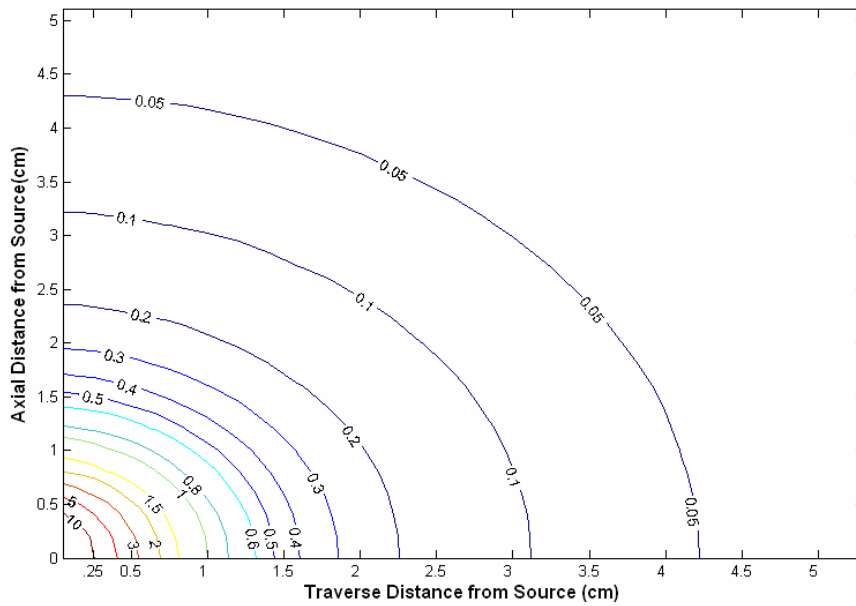
Figure 5.2.   Neutron isodose contours normalized as factors of the dose at the distance of 1 cm along the traverse axis of the source.

Table 5.1. Cf-252 transverse axis neutron absorbed dose rates (cGy/µg/h).

	Krishna--swamy -1972	Stoddard -1972	Windham et al -1972	Krishna--swamy -1974	Rivard -1999	This study*
Active length (cm)	2.0	2.0	2.0	0.4	point source	0.5
Distance (cm)						
0.5	4.93	5.00	5.14	8.772	8.295	7.814
1.0	1.72	1.60	1.751	2.196	2.064	2.047
1.5	0.83	0.75	0.846	0.953		0.905
2.0	0.485	0.45	0.459	0.524	0.495	0.498
2.5	0.314	0.30	0.293	0.331		0.309
3.0	0.207	0.205	0.197	0.216		0.208
3.5	0.144	0.145	0.1399	0.146		0.146
4.0	0.106	0.108	0.1030	0.109		0.107
4.5	0.082	0.070	0.0767	0.083		0.081
5.0	0.062	0.062	0.0600	0.064	0.0606	0.062
5.5			0.0472			0.055
6			0.0376			

* Statistical uncertainty less than 1%

Table 5.2. Cf-252 transverse axis gamma-ray absorbed dose rates (cGy/µg/h).

	Jones and Auxier -1972	Krishna--swamy -1972	Krishna--swamy -1974	This study*
Active length (cm)	2	2	0.4	0.5
Distance (cm)				
0.5		2.51	4.668	4.258
1.0	0.98	0.89	1.189	1.133
1.5		0.44	0.528	0.511
2.0	0.30	0.27	0.3	0.285
2.5		0.175	0.191	0.184
3.0	0.137	0.125	0.135	0.130
3.5		0.096	0.102	0.097
4.0		0.075	0.079	0.074
4.5		0.061	0.065	0.060
5.0		0.051	0.053	0.049
5.5				0.041

* Statistical uncertainty less than 1%

5.2 Measurement Results

The raw data from T1 and M1 ion chambers are displayed in Appendix B. Presented below in Figures 5.3 and 5.4 are the results of the dual ion chamber measurement compared with the results obtained from MCNP. The figures were created by processing the raw data in Appendix B from electrical charge to absorbed dose using equations 4.7 and 4.8. The absorbed doses thus obtained are that of A-150 plastic. To obtain the absorbed doses in water, these values were further multiplied by the kerma ratio of water to A-150 plastic. As shown in Fig. 5.3, the measured neutron absorbed doses at various distances are consistently lower by approximately 25% than the MCNP results. On the contrary, Fig. 5.4 shows that the measured gamma doses at various distances are consistently higher than the MCNP results. The differences between the two results are the greatest (~a factor of two) at the distance of 1 cm, and fall to approximately 30% at distances 2 cm and beyond. Each measured data point displayed on Figures 5.3 and 5.4 is the average of three measurements at each position. The fractional standard deviation at each position is at most approximately 1 %.

The overestimate of 25% of neutron dose rates by MCNP shown in Fig. 5.3 could be attributed to the uncertainty associated with the ^{252}Cf content in the Isotron source. It should be noted that the results of neutron dose obtained by MCNP are normalized to a single source neutron. To obtain the neutron dose rates shown in Fig. 5.3, one simply multiplies the MCNP results with the source neutron emission rate. It turns out that the neutron emission rate (or ^{252}Cf content) of the Isotron source was never accurately measured. The most accurate method for measuring neutron emission rate of a ^{252}Cf source is the Manganese Sulfate (MnSO$_4$) Bath Method, which is usually performed at the National Institute of Standard Technology (NIST) in Washington, D.C. While the ONRL-estimated ^{252}Cf content (used in this study) was based on a "NIST-traceable"
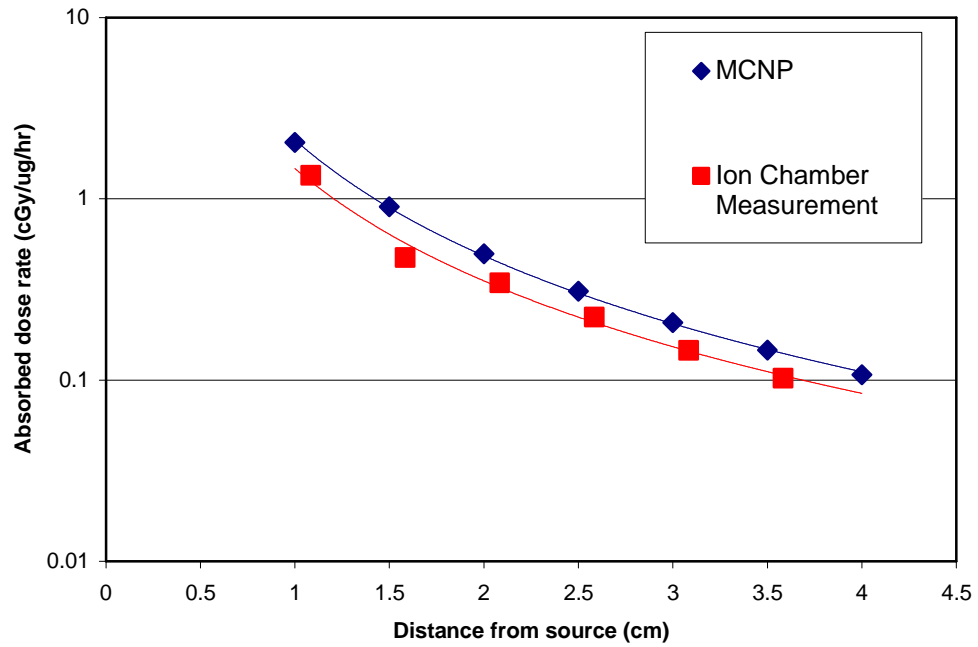
Figure 5.3. The transverse-axis neutron absorbed dose rate distribution in water: ion chamber measurements versus MCNP calculations.
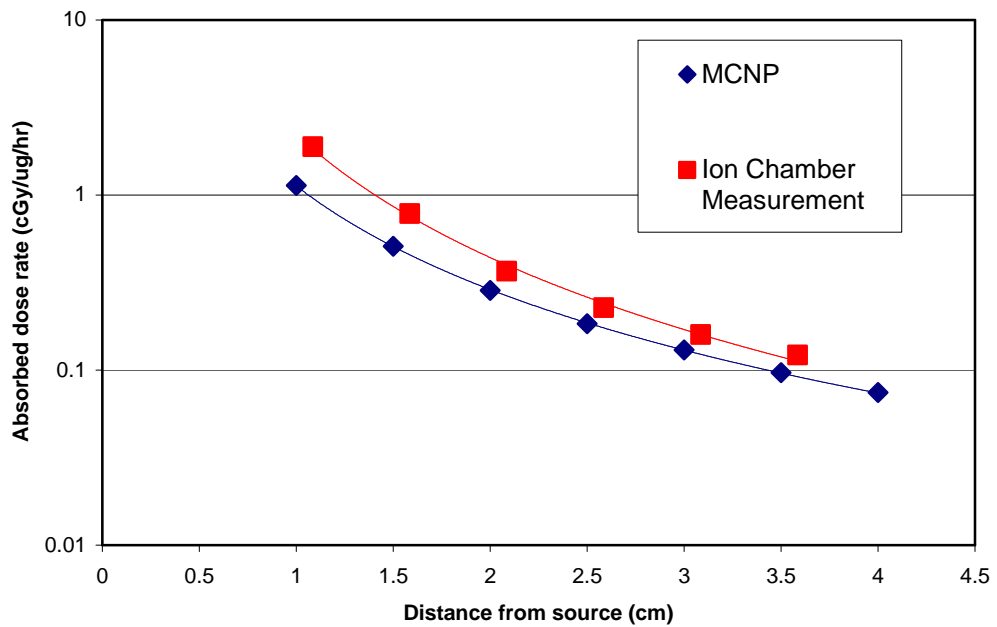
Figure 5.4. The transverse-axis gamma absorbed dose rate distribution in water: ion chamber measurements versus MCNP calculations.

^{252}Cf source, this source is an industry grade ^{252}Cf source which is much bigger in size than the Isotron source. The results of Fig. 5.3 indicate that the true ^{252}Cf content of the Isotron source used in this study is probably quite a bit lower than that estimated by ORNL. It should also be noted that had the Watt fission spectrum (instead of Maxwellian) be used in MCNP, the differences between the measured results and the MCNP results will be even greater (i.e. > 25%).

Similarly, the discrepancy between measured and MCNP-calculated gamma dose rates shown in Fig. 5.4 could be attributed to the uncertainties associated with the source gamma-ray emissions. The results of this study indicate that the Isotron source used in the experiment may contain significantly more low-energy gamma rays than the spectrum shown in Table 3.1. It is possible that these low-energy gamma rays (or x-rays) are emitted from the increasing amount of fission products as the source gets older. The above surmise is also supported by the finding that the measured gamma dose rates (shown in Fig. 5.4) are consistently greater than the measured neutron dose rates (shown in Fig. 5.3) at all distances from the source. This finding contradicts the results reported in the previous studies [8,14,15]. Specifically, the previous studies all show that the gamma dose rates are lower than neutron dose rates. The only reasonable explanation is that these low-energy gamma rays may have been effectively absorbed by the thick capsule wall of the much bigger sources used in the previous studies.

Finally, one must examine the experimental errors associated with the measured results. The errors associated with the ion chamber readings are typically between 5-10%. The errors on ion chamber positions are the highest at small distances, and they are estimated to be less than 10%. It turns out that the biggest contributor to the experimental error of dose rates is the unexpected change of source geometry during the experiment. This change of source geometry was discovered only after all the measurements were made. Specifically, Isotron source was developing a bend at the crimp between the source and the attached cable. Throughout the experiment, the

catheter itself was kept straight by the aluminum housing and by placing inside the catheter a steel rod in between measurements. Despite these efforts, a bend in the source meant that the system was no longer axially symmetric. To quantify this, a measurement was taken 1.085 cm away using the M1 detector while rotating the source 90 degrees. This rotation resulted in a 15% difference in charge collection. Carrying that difference through the data analysis resulted in approximately 20% error for the neutron dose and 15% error for the gamma dose. Additionally, assuming that the Isotron source was asymmetric at the time of the neutron measurements, this error could account almost entirely for the discrepancies in Figures 5.3 and 5.4 at distances close to the source. This does not however fully explain the differences between measured and calculated data farther than 2 cm away. This is because the source being bent is essentially a position error. Knowing that the source catheter is 3.1 mm in diameter with a smaller inner diameter, it is estimated that the source being bent can result in 1 to 1.5 mm error in position.

CHAPTER 6

CONCLUSIONS AND FUTURE WORK

Neutron and gamma dose rates in water surrounding the new medical grade ^{252}Cf brachytherapy source (the Isotron source) have been determined both by MCNP calculations and by ion-chamber measurements. The measured neutron absorbed dose rates were approximately 25% lower that predicted by MCNP for all dose positions. On the contrary, the measured gamma absorbed dose rates are higher than that predicted by MCNP. The discrepancies between the measured and calculated results cannot be accounted for by the experimental errors. The experimental results suggest that the true ^{252}Cf content of the Isotron source is approximately 25% less than the ORNL estimate and that the Isotron source emits significantly more low-energy gamma rays than the large ^{252}Cf sources (e.g. the AT source) used in the previous studies.

Because of the noted discrepancies/uncertainties of neutron and gamma dose rates, this study is deemed unsatisfactory. That is, before the Isotron source can be used for clinical trials the neutron and gamma dose rates in water must be more accurately determined. The following suggestions are made for that purpose.

1. Position error near the source (within 2 cm) must be greatly reduced or eliminated. To do so, the axial symmetry of the source must be strictly maintained throughout the experiment. It should be noted that 1 mm change in position correlates to a 15% change in dose rates.

2. The neutron emission rate (or ^{252}Cf content) of an Isotron source needs to be accurately determined at NIST using the Manganese Sulfate Bath Method.

3. Studies are needed to verify which of the two neutron spectra (Watt or Maxwellian) more accurately predicts neutron dose rates surrounding a Cf-252 source.

4. The primary gamma-ray spectrum of ^{252}Cf used in MCNP calculations needs to be more accurately modeled. A new model should include prompt fission gamma rays as well as the gamma rays emitted from fission products. This can be done using ORIGEN-S code (part of SCALE package) [17] and the fission yield data of ^{252}Cf. The current ORGEN-S code does not contain such data.

APPENDIX A

SAMPLE MCNP5 INPUT EXAMPLES

A.1 Neutron Dose Distribution Example

```
Title
C Neutron dose distribution in water phantom with Maxwellian source
C   CELL CARDS
C source cell cards**************************************
2 0 1000  -2000      IMP:N=1 $ gap space
3 4 -22.56  2000 -3000 IMP:N=1 $ casing
4 3 -15.4952  -1000  IMP:N=1 $ source
C 5  1 -1.0 3 -9999  IMP:N=1 $ water medium
9 0 9999           IMP:N=0 $ outside boundary
C top of source*****************************************
 100  2 -1 101 -102   1  -2 imp:n=1
 101  2 -1 101 -102   2  -3 imp:n=1
 102  2 -1 101 -102   3  -4 imp:n=1
 103  2 -1 101 -102   4  -5 imp:n=1
 104  2 -1 101 -102   5  -6 imp:n=1
 105  2 -1 101 -102   6  -7 imp:n=1
 106  2 -1 101 -102   7  -8 imp:n=1
 107  2 -1 101 -102   8  -9 imp:n=1
 108  2 -1 101 -102   9 -10 imp:n=1
 109  2 -1 101 -102  10 -11 imp:n=1
 110  2 -1 101 -102  11 -12 imp:n=1
 111  2 -1 101 -102  12 -13 imp:n=1
 112  2 -1 101 -102  13 -14 imp:n=1
 113  2 -1 101 -102  14 -15 imp:n=1
 114  2 -1 101 -102  15 -16 imp:n=1
 115  2 -1 101 -102  16 -17 imp:n=1
 116  2 -1 101 -102  17 -18 imp:n=1
 117  2 -1 101 -102  18 -19 imp:n=1
 118  2 -1 101 -102  19 -20 imp:n=1
 .
 . condensed for space
 .
 1350  2 -1 126 -127   1  -2 imp:n=1
 1351  2 -1 126 -127   2  -3 imp:n=1
 1352  2 -1 126 -127   3  -4 imp:n=1
 1353  2 -1 126 -127   4  -5 imp:n=1
 1354  2 -1 126 -127   5  -6 imp:n=1
 1355  2 -1 126 -127   6  -7 imp:n=1
 1356  2 -1 126 -127   7  -8 imp:n=1
 1357  2 -1 126 -127   8  -9 imp:n=1
 1358  2 -1 126 -127   9 -10 imp:n=1
 1359  2 -1 126 -127  10 -11 imp:n=1
 1360  2 -1 126 -127  11 -12 imp:n=1
 1361  2 -1 126 -127  12 -13 imp:n=1
```

```
 1362  2 -1 126 -127  13 -14 imp:n=1
 1363  2 -1 126 -127  14 -15 imp:n=1
 1364  2 -1 126 -127  15 -16 imp:n=1
 1365  2 -1 126 -127  16 -17 imp:n=1
 1366  2 -1 126 -127  17 -18 imp:n=1
 1367  2 -1 126 -127  18 -19 imp:n=1
 1368  2 -1 126 -127  19 -20 imp:n=1
C end of shells *****************************************
8 2 -1.0 -9999 127 imp:n=1
10 2 -1.0 -9999 -127 -1 101 imp:n=1
11 2 -1.0 20 -9999 -127 101 imp:n=1
12 2 -1.0 -101 3000 -9999 imp:n=1


C  SURFACE CARDS
C  Source terms
1000 RCC 0 0 -.25 0 0 .5 .025  $ source
2000 RCC 0 0 -.38 0 0 .76 .035 $ gap
3000 RCC 0 0 -.4 0 0 .8 .055   $ casing
9999 RCC 0 0 -10 0 0 20 10 $ outside boundary h=20cm and r=10cm
C planes ********************************
1 PZ -.01
2 PZ .01
3 PZ .24
4 PZ .26
5 PZ .49
6 PZ .51
7 PZ .99
8 PZ 1.01
9 PZ 1.49
10 PZ 1.51
11 PZ 1.99
12 PZ 2.01
13 PZ 2.49
14 PZ 2.51
15 PZ 2.99
16 PZ 3.01
17 PZ 3.49
18 PZ 3.51
19 PZ 3.99
20 PZ 4.01   $ end planes
C cylinders ****************************
101 CZ .24
102 CZ .26
103 CZ .49
104 CZ .51
105 CZ .74
106 CZ .76
107 CZ .99
108 CZ 1.01
109 CZ 1.49
110 CZ 1.51
111 CZ 1.99
112 CZ 2.01
113 CZ 2.49
114 CZ 2.51
115 CZ 2.99
```

```
116 CZ 3.01
117 CZ 3.49
118 CZ 3.51
119 CZ 3.99
120 CZ 4.01
121 CZ 4.4
122 CZ 4.6
123 CZ 4.9
124 CZ 5.1
125 CZ 5.4
126 CZ 5.6
127 CZ 5.9    $ end shells

C  MATERIALS
m2   1001.60c 2 8016.60c  1 $ water medium
mt2 lwtr.60
m3   46108.50c -2.5032 98252.60c -11.8556 8016.60c -1.1364 $ CF source
m4   77000.55c -10 78000.40c -90 $ Pt-10%Ir casing
SDEF ERG=D1 POS=0 0 0 CEL=4 RAD=D2 EXT=D3 AXS=0 0 1
SP1  -2  1.42 $ maxwellian fission spectrum
SI2 0 .024999
sp2 -21 0
SI3 0.24999
sp3 -21 0
F6:N 100 101 102 103 104 105 106 107 108 109 110 111 &
     112 113 114 115 116 117 118 150 151 152 153 154 &
    155 156 157 158 159 160 161 162  163  164   &
.
. condensed for space
.
   1304 1305  1306 1307 1308  1309  1310 1311 1312 1313 &
   1314 1315 1316 1317 1318 1350  1351  1352 1353  1354 1355 &
   1356 1357  1358 1359 1360  1361 1362  1363 1364 1365 1366 &
   1367 1368
nps  1e8
print
```

A.2 Primary Gamma Dose Distribution Example

Title
C CF-252 Gamma dose distribution in water phantom with default x-sec
C   CELL CARDS
C source cell cards**************************************
2 0 1000 -2000   IMP:p,e=1 $ gap space
3 4 -22.56 2000 -3000 IMP:p,e=1 $ casing
4 3 -15.4952 -1000 IMP:p,e=1 $ source
C 5 1 -1.0 3 -9999 IMP:p,e=1 $ water medium
9 0 9999   IMP:p,e=0 $ outside boundary
C top of source***
 100 2 -1 101 -102   1 -2 imp:p,e=1
 101 2 -1 101 -102   2 -3 imp:p,e=1
 102 2 -1 101 -102   3 -4 imp:p,e=1
 103 2 -1 101 -102   4 -5 imp:p,e=1
 104 2 -1 101 -102   5 -6 imp:p,e=1
 105 2 -1 101 -102   6 -7 imp:p,e=1
 106 2 -1 101 -102   7 -8 imp:p,e=1
 107 2 -1 101 -102   8 -9 imp:p,e=1
 108 2 -1 101 -102   9 -10 imp:p,e=1
 109 2 -1 101 -102 10 -11 imp:p,e=1
 110 2 -1 101 -102 11 -12 imp:p,e=1
 111 2 -1 101 -102 12 -13 imp:p,e=1
 112 2 -1 101 -102 13 -14 imp:p,e=1
 113 2 -1 101 -102 14 -15 imp:p,e=1
 114 2 -1 101 -102 15 -16 imp:p,e=1
 115 2 -1 101 -102 16 -17 imp:p,e=1
 116 2 -1 101 -102 17 -18 imp:p,e=1
 117 2 -1 101 -102 18 -19 imp:p,e=1
 118 2 -1 101 -102 19 -20 imp:p,e=1
.
. condensed for space
.
 1350 2 -1 126 -127   1 -2 imp:p,e=1
 1351 2 -1 126 -127   2 -3 imp:p,e=1
 1352 2 -1 126 -127   3 -4 imp:p,e=1
 1353 2 -1 126 -127   4 -5 imp:p,e=1
 1354 2 -1 126 -127   5 -6 imp:p,e=1
 1355 2 -1 126 -127   6 -7 imp:p,e=1
 1356 2 -1 126 -127   7 -8 imp:p,e=1
 1357 2 -1 126 -127   8 -9 imp:p,e=1
 1358 2 -1 126 -127   9 -10 imp:p,e=1
 1359 2 -1 126 -127 10 -11 imp:p,e=1
 1360 2 -1 126 -127 11 -12 imp:p,e=1
 1361 2 -1 126 -127 12 -13 imp:p,e=1
 1362 2 -1 126 -127 13 -14 imp:p,e=1
 1363 2 -1 126 -127 14 -15 imp:p,e=1
 1364 2 -1 126 -127 15 -16 imp:p,e=1
 1365 2 -1 126 -127 16 -17 imp:p,e=1
 1366 2 -1 126 -127 17 -18 imp:p,e=1
 1367 2 -1 126 -127 18 -19 imp:p,e=1

1368 2 -1 126 -127 19 -20 imp:p,e=1
C end of shells ***
8 2 -1.0 -9999 127 imp:p,e=1
10 2 -1.0 -9999 -127 -1 101 imp:p,e=1
11 2 -1.0 20 -9999 -127 101 imp:p,e=1
12 2 -1.0 -101 3000 -9999 imp:p,e=1

C SURFACE CARDS
C Source terms
1000 RCC 0 0 -.25 0 0 .5 .025 $ source
2000 RCC 0 0 -.38 0 0 .76 .035 $ gap
3000 RCC 0 0 -.4 0 0 .8 .055 $ casing
9999 RCC 0 0 -10 0 0 20 10 $ outside boundary h=20cm and r=10cm
C planes ********************************
1 PZ -.05
2 PZ .05
3 PZ .4
4 PZ .6
5 PZ .9
6 PZ 1.1
7 PZ 1.4
8 PZ 1.6
9 PZ 1.9
10 PZ 2.1
11 PZ 2.3
12 PZ 2.7
13 PZ 2.8
14 PZ 3.2
15 PZ 3.3
16 PZ 3.7
17 PZ 3.8
18 PZ 4.2
19 PZ 4.3
20 PZ 4.7 $ end planes
C cylinders **************************
101 CZ .24
102 CZ .26
103 CZ .45
104 CZ .55
105 CZ .9
106 CZ 1.1
107 CZ 1.4
108 CZ 1.6
109 CZ 1.9
110 CZ 2.1
111 CZ 2.4
112 CZ 2.6
113 CZ 2.9
114 CZ 3.1
115 CZ 3.3
116 CZ 3.7
117 CZ 3.8
118 CZ 4.2
119 CZ 4.3
120 CZ 4.7
121 CZ 4.8

```
122 CZ 5.2
123 CZ 5.3
124 CZ 5.7
125 CZ 5.8
126 CZ 5.9
127 CZ 6.0    $ end shells

C  MATERIALS
m2  1001 2 8016  1 $ water medium
m3  46108 -2.5032 98252 -11.8556 8016 -1.1364 $ CF source
m4  77000 -10 78000 -90 $ Pt-10%Ir casing
SDEF ERG=D1 POS=0 0 0 CEL=4 RAD=D2 EXT=D3 AXS=0 0 1
SI1 H .01 .05 .1 .2 .3 .4 .6 .8 1 1.33 1.66 2 2.5 3 4 5 6.5 8 10
sp1 D 0 7.3e5 1.613e3 2.515e3 3.54e6 7.587e3 5.242e-1 3.073e6 5.63e-2
    1.264e6 0 5.507e5 3.338e5 1.937e5 1.740e5 5.875e5 2.358e4 4.627e3 9.825e2
C probabilities from Cf-252 newsletter
SI2 0 .024999
sp2 -21 0
SI3 0.24999
sp3 -21 0
*F8:P 100 101 102 103 104 105 106 107 108 109 110 111 &
.
. condensed for space
.
  1367 1368
mode p e
nps  5e7
print
```

A.3 (Neutron, Gamma) Dose Distribution Example

```
Title
C CF-252 (n,Gamma) dose distribution in water phantom with default x-sec
C from maxwellian fission spectrum
C   CELL CARDS
C source cell cards*************************************
2 0 1000  -2000     IMP:n,p,e=1 $ gap space
3 4 -22.56  2000 -3000 IMP:n,p,e=1 $ casing
4 3 -15.4952  -1000  IMP:n,p,e=1 $ source
C 5  1 -1.0 3 -9999  IMP:n,p,e=1 $ water medium
9 0 9999          IMP:n,p,e=0 $ outside boundary
C top of source*****************************************
 100  2 -1 101 -102   1  -2 imp:n,p,e=1
 101  2 -1 101 -102   2  -3 imp:n,p,e=1
 102  2 -1 101 -102   3  -4 imp:n,p,e=1
 103  2 -1 101 -102   4  -5 imp:n,p,e=1
 104  2 -1 101 -102   5  -6 imp:n,p,e=1
 105  2 -1 101 -102   6  -7 imp:n,p,e=1
 106  2 -1 101 -102   7  -8 imp:n,p,e=1
 107  2 -1 101 -102   8  -9 imp:n,p,e=1
 108  2 -1 101 -102   9 -10 imp:n,p,e=1
 109  2 -1 101 -102  10 -11 imp:n,p,e=1
 110  2 -1 101 -102  11 -12 imp:n,p,e=1
 111  2 -1 101 -102  12 -13 imp:n,p,e=1
 112  2 -1 101 -102  13 -14 imp:n,p,e=1
 113  2 -1 101 -102  14 -15 imp:n,p,e=1
 114  2 -1 101 -102  15 -16 imp:n,p,e=1
 115  2 -1 101 -102  16 -17 imp:n,p,e=1
 116  2 -1 101 -102  17 -18 imp:n,p,e=1
 117  2 -1 101 -102  18 -19 imp:n,p,e=1
 118  2 -1 101 -102  19 -20 imp:n,p,e=1
 .
 . condensed for space
 .
 1350 2 -1 126 -127   1  -2 imp:n,p,e=1
 1351 2 -1 126 -127   2  -3 imp:n,p,e=1
 1352 2 -1 126 -127   3  -4 imp:n,p,e=1
 1353 2 -1 126 -127   4  -5 imp:n,p,e=1
 1354 2 -1 126 -127   5  -6 imp:n,p,e=1
 1355 2 -1 126 -127   6  -7 imp:n,p,e=1
 1356 2 -1 126 -127   7  -8 imp:n,p,e=1
 1357 2 -1 126 -127   8  -9 imp:n,p,e=1
 1358 2 -1 126 -127   9 -10 imp:n,p,e=1
 1359 2 -1 126 -127  10 -11 imp:n,p,e=1
 1360 2 -1 126 -127  11 -12 imp:n,p,e=1
 1361 2 -1 126 -127  12 -13 imp:n,p,e=1
 1362 2 -1 126 -127  13 -14 imp:n,p,e=1
 1363 2 -1 126 -127  14 -15 imp:n,p,e=1
 1364 2 -1 126 -127  15 -16 imp:n,p,e=1
 1365 2 -1 126 -127  16 -17 imp:n,p,e=1
 1366 2 -1 126 -127  17 -18 imp:n,p,e=1
```

```
 1367  2 -1 126 -127  18 -19 imp:n,p,e=1
 1368  2 -1 126 -127  19 -20 imp:n,p,e=1
C end of shells *****************************************
8 2 -1.0 -9999 127          imp:n,p,e=1
10 2 -1.0 -9999 -127 -1 101  imp:n,p,e=1
11 2 -1.0 20 -9999 -127 101  imp:n,p,e=1
12 2 -1.0 -101 3000 -9999    imp:n,p,e=1

C  SURFACE CARDS
C  Source terms
1000 RCC 0 0 -.25 0 0 .5 .025  $ source
2000 RCC 0 0 -.38 0 0 .76 .035 $ gap
3000 RCC 0 0 -.4 0 0 .8 .055   $ casing
9999 RCC 0 0 -10 0 0 20 10 $ outside boundary h=20cm and r=10cm
C planes ********************************
1 PZ -.05
2 PZ .05
3 PZ .4
4 PZ .6
5 PZ .9
6 PZ 1.1
7 PZ 1.4
8 PZ 1.6
9 PZ 1.9
10 PZ 2.1
11 PZ 2.3
12 PZ 2.7
13 PZ 2.8
14 PZ 3.2
15 PZ 3.3
16 PZ 3.7
17 PZ 3.8
18 PZ 4.2
19 PZ 4.3
20 PZ 4.7   $ end planes
C cylinders **************************
101 CZ .24
102 CZ .26
103 CZ .45
104 CZ .55
105 CZ .9
106 CZ 1.1
107 CZ 1.4
108 CZ 1.6
109 CZ 1.9
110 CZ 2.1
111 CZ 2.4
112 CZ 2.6
113 CZ 2.9
114 CZ 3.1
115 CZ 3.3
116 CZ 3.7
117 CZ 3.8
118 CZ 4.2
119 CZ 4.3
120 CZ 4.7
```

```
121 CZ 4.8
122 CZ 5.2
123 CZ 5.3
124 CZ 5.7
125 CZ 5.8
126 CZ 5.9
127 CZ 6.0    $ end shells

C  MATERIALS
m2  1001 2 8016  1 $ water medium
mt2 lwtr.60
m3  46108 -2.5032 98252 -11.8556 8016 -1.1364 $ CF source
m4  77000 -10 78000 -90 $ Pt-10%Ir casing
SDEF ERG=D1 POS=0 0 0 CEL=4 RAD=D2 EXT=D3 AXS=0 0 1
SP1  -2  1.42 $ maxwellian fission spectrum
SI2 0 .024999
sp2 -21 0
SI3 0.24999
sp3 -21 0
*F8:P 100 101 102 103 104 105 106 107 108 109 110 111 &
.
. condensed for space
.
   1367 1368
mode n p e
nps  5e7
print
```

APPENDIX B

MEASUREMENT DATA

Table B.1. T1 measurement data from 11/29/07.

Transverse Caliper Reading (mm)	Axial Caliper Reading (mm)	Charge 300 sec (pC)	Temp deg F	Humidity	Time	Mean Charge (pC)	Deviation (pC)	Standard Deviation (pC)
139.8	104.0	92.65	74.9	33.0	7:47	92.9500	-0.3000	0.2750
		93.01	75.5	33.6	8:32		0.0600	
		93.19	75.3	33.7	8:38		0.2400	
129.8	104.0	20.83	75.3	34.9	8:48	20.7300	0.1000	0.0866
		20.68	75.3	34.7	8:54		-0.0500	
		20.68	75.4	34.4	8:59		-0.0500	
119.8	104.0	9.20	75.3	34.6	9:06	9.2833	-0.0833	0.0764
		9.30	75.4	35.3	9:12		0.0167	
		9.35	75.3	34.7	9:17		0.0667	
109.8	104.0	5.61	75.3	34.3	9:24	5.5800	0.0300	0.0265
		5.57	75.2	35.1	9:30		-0.0100	
		5.56	75.3	35.0	9:35		-0.0200	
99.8	104.0	3.77	75.5	34.9	9:41	3.7500	0.0200	0.0346
		3.71	75.3	34.4	9:47		-0.0400	
		3.77	75.4	34.7	9:52		0.0200	
104.8	104.0	4.48	75.4	35.0	9:59	4.5133	-0.0333	0.0351
		4.55	75.4	34.9	10:04		0.0367	
		4.51	75.4	35.2	10:10		-0.0033	
114.8	104.0	7.01	75.3	34.7	10:15	7.0067	0.0033	0.0252
		7.03	75.4	36.0	10:21		0.0233	
		6.98	75.4	35.4	10:27		-0.0267	
124.8	104.0	13.38	75.5	36.3	10:32	13.3567	0.0233	0.0586
		13.40	75.5	36.8	10:38		0.0433	
		13.29	75.6	36.6	10:43		-0.0667	
139.8	99.0	75.44	76.4	34.7	12:27	75.2700	0.1700	0.1752
		75.28	76.6	35.8	12:33		0.0100	
		75.09	76.5	37.2	12:38		-0.1800	
134.8	99.0	33.18	76.2	38.0	12:51	33.3400	-0.1600	0.1769
		33.53	76.1	37.9	12:56		0.1900	
		33.31	76.2	37.8	13:01		-0.0300	

134.8	104.0	36.70	75.8	38.2	13:07	36.6400	0.0600	0.0794
		36.55	75.8	38.6	13:12		-0.0900	
		36.67	75.8	38.6	13:17		0.0300	
129.8	99.0	19.23	75.7	38.5	13:23	19.2100	0.0200	0.0200
		19.21	75.8	38.3	13:28		0.0000	
		19.19	75.9	38.5	13:33		-0.0200	
119.8	99.0	9.37	75.8	38.5	13:40	9.2767	0.0933	0.0950
		9.18	76.1	38.7	13:45		-0.0967	
		9.28	76.1	38.4	13:50		0.0033	
119.8	94.0	8.82	76.0	38.3	13:55	8.7933	0.0267	0.0833
		8.86	76.0	38.2	14:00		0.0667	
		8.70	76.1	38.1	14:05		-0.0933	
129.8	94.0	16.65	76.1	38.0	14:11	16.6467	0.0033	0.0153
		16.63	75.8	38.3	14:16		-0.0167	
		16.66	75.7	38.3	14:21		0.0133	
139.8	94.0	44.67	75.7	38.1	14:27	44.6233	0.0467	0.0451
		44.58	75.7	38.0	14:32		-0.0433	
		44.62	75.7	38.3	14:37		-0.0033	
139.8	84.0	17.55	75.6	38.3	14:43	17.5100	0.0400	0.0608
		17.54	75.9	38.1	14:49		0.0300	
		17.44	76.0	37.9	14:54		-0.0700	
129.8	84.0	10.83	76.0	37.8	14:59	10.8500	-0.0200	0.0200
		10.87	76.1	38.1	15:04		0.0200	
		10.85	76.3	37.6	15:09		0.0000	
109.8	84.0	4.73	76.2	37.5	15:15	4.7400	-0.0100	0.0361
		4.71	76.1	38.0	15:20		-0.0300	
		4.78	76.0	37.8	15:26		0.0400	
11/29/2007 Background Measurements	600 second Charge	1.40				1.2967	0.1033	0.1050
		1.19					-0.1067	
		1.30					0.0033	

Table B.2. T1 measurement data from 11/30/07.

Transverse Caliper Reading (mm)	Axial Caliper Reading (mm)	Charge 300 sec (pC)	Temp deg F	Humidity	Time	Mean Charge (pC)	Deviation (pC)	Standard Deviation (pC)
134.8	94.0	23.64	75.2	30.0	7:39	23.7100	-0.0700	0.0889
		23.68	75.3	29.3	7:45		-0.0300	
		23.81	75.5	28.9	7:50		0.1000	
124.8	94.0	10.96	75.7	28.8	7:56	11.0800	-0.1200	0.1200
		11.20	75.7	28.6	8:01		0.1200	
		11.08	75.7	28.5	8:06		0.0000	
114.8	94.0	6.40	75.9	28.5	8:12	6.4867	-0.0867	0.0751
		6.53	75.9	28.6	8:17		0.0433	
		6.53	76.0	28.4	8:22		0.0433	
114.8	99.0	6.95	76.1	28.3	8:29	6.9467	0.0033	0.0153
		6.96	76.1	28.2	8:34		0.0133	
		6.93	75.6	28.7	8:39		-0.0167	
124.8	99.0	12.56	75.9	28.4	8:57	12.6200	-0.0600	0.0656
		12.69	76.2	28.2	9:02		0.0700	
		12.61	76.2	28.2	9:07		-0.0100	
114.8	89.0	6.07	76.2	28.3	9:13	6.1167	-0.0467	0.0451
		6.16	76.3	28.5	9:18		0.0433	
		6.12	76.3	28.4	9:23		0.0033	
119.8	89.0	7.76	76.3	28.5	9:29	7.7733	-0.0133	0.0153
		7.79	76.3	28.3	9:34		0.0167	
		7.77	76.4	28.4	9:39		-0.0033	
124.8	89.0	10.05	76.4	28.6	9:46	10.0833	-0.0333	0.0416
		10.07	76.6	28.6	9:51		-0.0133	
		10.13	76.5	28.6	9:56		0.0467	
129.8	89.0	13.23	76.5	28.7	10:02	13.1933	0.0367	0.0473
		13.14	76.5	28.8	10:07		-0.0533	
		13.21	76.5	29.2	10:12		0.0167	
134.8	89.0	17.70	76.5	29.3	10:17	17.7633	-0.0633	0.0551
		17.79	76.5	29.5	10:23		0.0267	
		17.80	76.4	29.5	10:28		0.0367	
139.8	89.0	24.48	76.3	29.7	10:34	24.3900	0.0900	0.1082
		24.27	76.4	29.8	10:42		-0.1200	
		24.42	76.3	29.8	10:47		0.0300	
134.8	84.0	12.99	76.5	31.0	10:53	12.9833	0.0067	0.0404
		13.02	76.5	30.6	10:59		0.0367	
		12.94	76.6	30.5	11:04		-0.0433	
124.8	84.0	8.49	76.8	30.9	11:11	8.5033	-0.0133	0.0231
		8.53	76.8	30.6	11:16		0.0267	
		8.49	76.6	30.5	11:21		-0.0133	
119.8	84.0	6.84	76.8	30.9	13:10	6.8333	0.0067	0.0208
		6.85	77.0	30.7	13:16		0.0167	
		6.81	76.9	30.8	13:21		-0.0233	
11/30/2007 Background Measurements	600 second Charge	1.42				1.3600	0.0600	0.1039
		1.42					0.0600	
		1.24					-0.1200	

Table B.3. M1 measurement data from 12/17/07.

Transverse Caliper Reading (mm)	Axial Caliper Reading (mm)	Charge 300 sec (pC)	Temp deg F	Humidity	Time	Mean Charge (pC)	Deviation (pC)	Standard Deviation (pC)
138.50	108.00	67.41	72.3	29.2	10:51	67.5400	-0.1300	0.1179
		67.64	72.2	30.5	10:56		0.1000	
		67.57	72.1	30.9	11:02		0.0300	
138.50	103.00	49.17	72.1	30.0	11:11	49.2500	-0.0800	0.0985
		49.36	71.9	30.8	11:16		0.1100	
		49.22	72.3	31.2	11:21		-0.0300	
138.50	98.00	26.69	72.5	30.0	11:33	26.7367	-0.0467	0.0503
		26.73	72.4	30.1	11:39		-0.0067	
		26.79	72.5	29.7	11:44		0.0533	
138.50	93.00	15.13	72.4	30.9	11:51	15.0900	0.0400	0.0361
		15.08	72.3	30.7	11:56		-0.0100	
		15.06	72.5	30.6	12:01		-0.0300	
138.50	88.00	9.78	72.3	31.2	12:08	9.7500	0.0300	0.0265
		9.73	72.6	31.2	12:13		-0.0200	
		9.74	72.4	31.1	12:18		-0.0100	
133.50	88.00	8.38	72.5	30.8	12:24	8.3633	0.0167	0.0153
		8.35	72.5	31.2	12:30		-0.0133	
		8.36	72.6	31.1	12:35		-0.0033	
133.50	93.00	11.66	72.7	31.4	12:41	11.6800	-0.0200	0.0265
		11.67	72.8	31.5	12:46		-0.0100	
		11.71	72.9	31.2	12:52		0.0300	
133.50	98.00	16.99	72.6	31.4	12:58	17.0167	-0.0267	0.0551
		17.08	72.6	31.4	13:03		0.0633	
		16.98	72.8	31.2	13:09		-0.0367	
133.50	103.00	23.97	72.7	31.2	13:15	24.0400	-0.0700	0.0608
		24.08	72.7	31.1	13:20		0.0400	
		24.07	72.9	31.1	13:25		0.0300	
133.50	108.00	28.12	72.6	30.9	13:31	28.1667	-0.0467	0.1172
		28.08	72.9	30.8	13:39		-0.0867	
		28.30	72.7	30.9	13:44		0.1333	
128.50	108.00	13.50	72.5	31.1	13:50	13.5567	-0.0567	0.0513
		13.60	72.8	31.2	13:55		0.0433	
		13.57	72.9	31.2	14:00		0.0133	
128.50	103.00	12.64	73.0	31.3	14:06	12.6333	0.0067	0.0702
		12.70	72.8	31.2	14:11		0.0667	
		12.56	72.8	31.3	14:16		-0.0733	
128.50	98.00	10.66	72.9	31.3	14:22	10.6367	0.0233	0.0208
		10.63	72.9	31.2	14:27		-0.0067	
		10.62	72.8	31.3	14:32		-0.0167	
128.50	93.00	8.56	72.9	30.5	14:37	8.5333	0.0267	0.0737
		8.59	72.6	30.9	14:42		0.0567	
		8.45	73.0	30.6	14:47		-0.0833	
128.50	88.00	6.86	73.0	30.9	14:53	6.8267	0.0333	0.0306
		6.82	73.1	30.5	14:58		-0.0067	
		6.80	72.9	30.8	15:03		-0.0267	

123.50	88.00	5.53	73.1	30.5	15:09	5.5500	-0.0200	0.0265
		5.58	73.1	31.0	15:14		0.0300	
		5.54	73.0	31.0	15:19		-0.0100	
123.50	93.00	6.53	73.1	31.3	15:26	6.5333	-0.0033	0.0252
		6.51	73.3	31.4	15:31		-0.0233	
		6.56	73.1	31.6	15:36		0.0267	
123.50	98.00	7.53	73.1	31.3	15:42	7.5367	-0.0067	0.0208
		7.56	73.3	30.6	15:48		0.0233	
		7.52	72.9	30.7	15:53		-0.0167	
12/17/2007 Background Measurements	600 second Charge	0.93				0.9867	-0.0567	0.0551
		0.99					0.0033	
		1.04					0.0533	

Table B.4. M1 measurement data from 12/18/07.

Transverse Caliper Reading (mm)	Axial Caliper Reading (mm)	Charge 300 sec (pC)	Temp deg F	Humidity	Time	Mean Charge (pC)	Deviation (pC)	Standard Deviation (pC)
123.50	103.00	7.93	72.9	30.7	10:50	7.9200	0.0100	0.0173
		7.90	72.6	30.7	10:55		-0.0200	
		7.93	72.9	30.9	11:02		0.0100	
123.50	108.00	8.26	72.7	30.8	11:08	8.2633	-0.0033	0.0153
		8.25	72.9	31.0	11:13		-0.0133	
		8.28	72.7	31.2	11:19		0.0167	
118.50	108.00	5.78	72.7	31.6	11:25	5.8367	-0.0567	0.0666
		5.82	72.8	31.7	11:30		-0.0167	
		5.91	72.8	32.0	11:35		0.0733	
118.50	103.00	5.70	72.7	32.0	11:42	5.6900	0.0100	0.0265
		5.66	72.6	31.9	11:47		-0.0300	
		5.71	72.7	32.6	11:52		0.0200	
118.50	98.00	5.31	72.6	31.6	11:58	5.2667	0.0433	0.0379
		5.25	72.9	32.2	12:03		-0.0167	
		5.24	72.8	32.3	12:08		-0.0267	
118.50	93.00	4.83	72.6	32.1	12:14	4.7767	0.0533	0.0757
		4.81	72.6	32.6	12:19		0.0333	
		4.69	72.8	31.6	12:32		-0.0867	
118.50	88.00	4.19	72.6	32.2	13:52	4.1500	0.0400	0.0529
		4.09	72.8	31.7	13:58		-0.0600	
		4.17	72.6	31.6	14:05		0.0200	
113.50	88.00	3.43	72.8	32.6	14:13	3.4100	0.0200	0.0346
		3.37	72.9	32.6	14:20		-0.0400	
		3.43	72.5	32.5	14:25		0.0200	
113.50	93.00	3.83	72.9	33.2	14:49	3.8000	0.0300	0.0436
		3.75	72.8	32.8	14:54		-0.0500	
		3.82	72.7	32.7	15:00		0.0200	
113.50	98.00	4.16	72.7	33.0	15:06	4.1433	0.0167	0.0208
		4.12	72.7	32.6	15:11		-0.0233	
		4.15	72.8	32.9	15:16		0.0067	
113.50	103.00	4.33	72.7	32.8	15:22	4.3567	-0.0267	0.0643
		4.31	72.9	32.9	15:27		-0.0467	
		4.43	72.8	32.9	15:32		0.0733	
113.50	108.00	4.45	72.9	32.6	15:38	4.4767	-0.0267	0.0379
		4.46	72.8	33.0	15:43		-0.0167	
		4.52	72.9	32.7	15:48		0.0433	
12/18/2007 Background Measurements	600 second Charge	0.28				0.3033	-0.0233	0.0252
		0.33					0.0267	
		0.30					-0.0033	

REFERENCES

1. Maruyama, Y. et al. "CF-252 Neutron Brachytherapy Treatment for Cure of Cervical Cancer," Nucl Sci Appl, vol. 4, pp. 181-192, 1991.

2. Zhao, H. et al. "Clinical Report on External Irradiation Combined with Californium-252 Neutrons Intraluminal Brachytherapy for Cervical Carcinoma Treatment," Tumori, vol. 93, pp. 636 – 640, 2007.

3. ORNL Invention Disclosure No. 1289, under CRADA contract with Isotron, 2002.

4. X-5 Monte Carlo Team, MCNP – A General Monte Carlo N-Particle Transport Code, Version 5, Los Alamos report LA-UR-03-1987, 2003.

5. ICRU Report 26, "Neutron Dosimetry for Biology and Medicine," International Commission on Radiation Units and Measurements, Washington, D.C., 1977.

6. Martin, R.C. Californium-252 Newsletter, 4, 1 Oak Ridge National Laboratory, January 2000.

7. McGarry, E.D. and Boswell, W. "NBS Measurement Services: Neutron Source Strength Calibrations," Library of Congress Catalog Card Number: 88-600510, U.S. Government Printing Office, Washington, D.C., 1988.

8. Rivard, M.J. "Dosimetry for ^{252}Cf Neutron Emitting Brachytherapy Sources: Protocol, measurements, and calculations," Med Phys, Vol. 26 (8), pp. 1503-1514, 1999.

9. Märten, H. et al. "The ^{252}Cf(sf) Neutron Spectrum in the 5- to 20-MeV Energy Range," Nucl. Sci. Eng., Vol. 106, pp. 353-366, 1990.

10. Chalupka, R.D. et al. "Results of a Low Background Measurement of the New Fission Neutron Spectrum from ^{252}Cf in the 9- to 29-MeV Energy Range," Nucl. Sci. Eng., vol. 106, pp. 367-376, 1990.

11. Attix, F.H., *Introduction to Radiological Physics and Radiation Dosimetry*, pp 475-480, John Wiley & Sons, Inc., 1986.

12. Zhang, X., Development and Validation of a Nanodosimetry-Based Cell Survival Model for Mixed High- and Low-LET Radiations, PhD Thesis, Georgia Tech, August 2006.

13. ICRU Report 45, "Clinical Neutron Dosimetry, Part 1: Determination of Absorbed Dose in a Patient Treated by External Beams of Fast Neutrons," International Commission on Radiation Units and Measurements, Bethesda, Maryland, 1989.

14. Anderson, L.L., "Status of Dosimetry for ^{252}Cf Medical Neutron Sources," Phys. Med. Biol., Vol. 18 (6), pp. 779-799, 1973.

15. Krishnaswamy, V., "Calculated Depth Dose Tables for Californium-252 Seed Source in Tissue," Phys. Med. Biol., Vol. 19 (6), pp. 886-888, 1974.

16. Stoddard, D.H. and Hootman, H.E., "Cf-252 Shielding Guide," Savannah River Laboratory Report DP-1246, 1971.

17. SCALE: A Modular Code System for Performing Standardized Computer Analyses for Licensing Evaluation. ORNL/TM-2005/39, Version 5.1, Vols. I-III, Nov 2006.